USING COMPUTED TOMOGRAPHY SCANNING TECHNOLOGY TO EXTRACT VIRTUAL WOOD CORES, DERIVE WOOD DENSITY RADIAL PATTERNS, AND TEST HYPOTHESES ABOUT DIRECTION, CORE SIZE, AND YEAR OF GROWTH

*J. Beaulieu**

Scientist Emeritus
Natural Resources Canada
Canadian Forest Service
Canadian Wood Fibre Centre
Sainte-Foy Station, Québec, Québec, Canada
and
Invited Professor
Département des sciences du bois et de la forêt
Faculté de foresterie, de géographie et de géomatique
Université Laval
Québec, Québec, Canada
E-mail: jean.beaulieu@canada.ca

L. Han

Research Assistant
E-mail: liwen.han@mcgill.ca

P. Dutilleul

Professor
Department of Plant Science
McGill University, Macdonald Campus
Ste-Anne-de-Bellevue, Québec, Canada
E-mail: pierre.dutilleul@mcgill.ca

(Received February 2016)

Abstract. Computed tomography (CT) scanning technology was used to collect millions of three-dimensional data called CT numbers on eight white spruce (*Picea glauca* [Moench] Voss) wood disks classified as small or medium on the basis of the relevant field of view. The collected data were then converted to wood density estimates using a calibration equation. Virtual wood cores of three sizes (diameters of 1 voxel, which is the smallest volumetric unit on which a CT number is computed, 5 mm, and 12 mm) were extracted in four orthogonal directions from pith to bark. This made the assessment of the effects of direction and core size on the wood density estimates possible. The averaged values and radial patterns of wood density as estimated from CT scanning data were found to be typical of the values and patterns reported for the white spruce tree species in the literature, especially in relation to the year of growth because the experimental trees varied in age. In conclusion, the application of CT scanning technology in wood science allows the digital extraction of three-dimensional data subsets to perform wood density estimation, radial pattern analysis, and hypothesis testing, and the results are valuable complements to those obtained with other technologies such as X-ray densitometry.

Keywords: Wood density, computed tomography scanning, virtual wood cores, radial pattern, white spruce (*Picea glauca* [Moench] Voss).

INTRODUCTION

Wood is a versatile raw material that enters into the manufacturing of a variety of end-use products.

* Corresponding author

Compared with other materials such as concrete and steel, it has the advantages of originating from a renewable resource, generating fewer greenhouse gases, and requiring less energy during its transformation (Upton et al 2008). Wood properties are known to vary among species, between trees within species, and both vertically and along the radial axis inside the stem (Zobel and van Buijtenen 1989; Manceur et al 2012). Activity in vascular cambium beneath the bark and modification of wood cells during the differentiation phase generate variation that is eventually observed in wood properties (Zobel and van Buijtenen 1989; Larson 1994; Plomion et al 2001). For coniferous species such as spruces (Corriveau et al 1991; Yanchuk and Kiss 1993; Lenz et al 2011), radiata pine (*Pinus radiata* D. Don), and loblolly pine (*Pinus taeda* L.) (Myszewski et al 2004; Kumar et al 2006; Baltunis et al 2007), the analysis of wood properties has indeed shown variation in mechanical properties such as stiffness and related traits, including wood density and microfibril angle. Anatomical characteristics (eg cellular dimensions, wall thickness, fiber coarseness), which are important for the pulp and paper industry (Kibblewhite 1999), also show an important level of variation (Ivkovich et al 2002b; Beaulieu 2003).

Variation in wood properties and most quantitative traits (eg tree height and diameter) is because of many controlling genes with small effects (Ivkovich et al 2002a; Lenz et al 2010; Beaulieu et al 2011). Wood properties are also influenced by environmental factors (Cown et al 1991; Lenz et al 2014) and can be manipulated by silvicultural treatments to some extent (MacDonald and Hubert 2002). The knowledge of wood properties is central to the optimization of the forest product value chain (MacKenzie and Bruemmer 2009). Ideally, wood properties are assessed during the transformation processes. However, it is often essential to assess wood properties before trees are harvested, using nondestructive methods (Bucur 2003). This is true especially for studies in which standing trees must be kept alive for reproduction purposes or simply because they are still too young to be harvested.

One of the most popular procedures to nondestructively assess the wood properties of standing trees, in particular wood density and microfibril angle, consists of collecting wood cores generally at breast height and then using technologies such as SilviScan™ (Evans and Ilic 2001) and X-ray densitometry combined with X-ray diffractometry (Beaulieu et al 2014). However, all trees do not present a circular growth of the stem (Dutilleul et al 2014), and this can be because of causes as varied as exposition to strong prevailing wind, upward bending caused by gravity forces affecting leaning trees, and localization on a slope, which favors the production of reaction wood (Sinnott 1952; UK Forest Commission 2005), as well as damage by biotic or abiotic adverse factors, competition from neighbors, etc. It follows that if only one wood core is collected at a given height in a tree stem to estimate some wood property, a question naturally arises: Is a wood property estimated in this way representative of the whole stem, only the height considered, or an even smaller part of the stem at that height (ie a number of growth rings in the relevant direction)? Also, because wood cores with a diameter of 5 or 12 mm are usually taken from stems of standing trees, it would be very useful to know if both core sizes allow similar estimation of wood properties and to assess the variability of estimates in relation to core size.

For this study, we submitted wood disks of white spruce (*Picea glauca* [Moench] Voss) to high-resolution X-ray computed tomography (CT) scanning. We digitally extracted virtual cores of various sizes (diameters) from the three-dimensional (3-D) array of CT scanning data collected for each wood disk. The production and availability of these virtual cores allowed us to address a total of four research questions. Specifically, our objectives were to test that 1) wood density estimates are direction-dependent, 2) average estimated wood density is a function of year of growth, 3) variation in estimated wood density from pith to bark changes with the sampling direction, ie the radial pattern of fluctuations in estimated wood density differs among sampling directions, and 4) wood density estimates

vary with wood core size. Our central goal was to demonstrate that results obtained with this approach are similar to those reported in the literature, which were obtained with traditional means and possibly with more than one approach because of practical constraints.

MATERIALS AND METHODS

Data Collection

Wood disks were collected from the stems of eight white spruce (*P. glauca* [Moench] Voss) trees for this study. These trees had been harvested during an ecological survey conducted by the Ministère des Ressources naturelles du Québec in the southern Quebec forest region between September and November 2009. The sampled trees were from three ecological regions, ie the maple–yellow birch, balsam fir–yellow birch, and spruce–moss bioclimatic domains (latitudes between 45.44°N and 50.89°N and longitudes between 64.19°W and 79.08°W). Among the eight wood disks that were retained (one per tree), five had diameters of about 15-17 cm (including the bark) and are called small-size wood disks and coded S1-S5 hereafter, whereas the three other disks, which will be referred to as medium-size wood disks and M1-M3, had diameters of about 24-26 cm (including the bark). They were air-dried after collection and kept indoors until their shipment to the CT Scanning Laboratory for Agricultural and Environmental Research at the Macdonald Campus of McGill University in Ste-Anne-de-Bellevue, QC.

The eight wood disks were entirely scanned with a Toshiba Xvision high-resolution X-ray CT scanner (Toshiba Corporation, Medical Systems Division, Tokyo, Japan), the same that was used for the wood CT scanning studies reported in Manceur et al (2012) and Dutilleul et al (2014). A summary of the general principles is subsequently presented, together with aspects specific to this study. An X-ray absorption coefficient (also known as the linear attenuation coefficient) was calculated for each voxel (a volumetric unit, the 3-D extension of a pixel) within each slice of the CT-scanned object (a wood disk). The X-ray absorption coefficient was then converted to a CT number (CTN), expressed in Hounsfield units (HU) (Kalender 2000):

$$\mathrm{CTN} = \frac{\mu_{\mathrm{object}} - \mu_{\mathrm{water}}}{\mu_{\mathrm{object}} - \mu_{\mathrm{air}}} \times 1000,$$

where μ_{object} is the X-ray absorption coefficient for 1 voxel of the CT-scanned object, μ_{water} is the X-ray absorption coefficient for pure water (ie 0-HU CTN), and μ_{air} is the null X-ray absorption coefficient of pure air (ie −1000-HU CTN by calibration). Thus, negative CTN values correspond to voxels less dense than water, and positive CTN values correspond to voxels denser than water. All the CTN values computed for a CT image with a given thickness were saved in a 512 × 512 matrix. Only the wood part of the CT images (excluding air and bark) was used in further data analyses.

Our wood disks were CT scanned using the following configuration parameter values: 50 mA (tube current), 120 kV (tube voltage), 1 mm (X-ray beam width), and 18 or 24 cm (SS or S field of view in CT-scanning terminology) for the small- and medium-size wood disks, respectively; no zoom factor was applied. Also, the Helical Scan option was used because it allows, thanks to advanced interpolations, multiple image reconstructions from CT-scanning data collected in one rotation and provides enhanced image precision (Han et al 2008). Accordingly, CT images (*x*-*y* plane), which are maps of CTN values, were constructed every 0.3 mm along the tree stem (*z* axis). Further details about the scanning technology and its application in a wood science study can be found in Manceur et al (2012).

The CTN values thus obtained were converted into wood density estimates, using the calibration equation of Lindgren (1991) for not oven-dried wood samples: $D = 1015 + 0.993$ CTN, where D is the wood density (expressed in kg/m^3). Freyburger et al (2009) showed that MC has limited effects on the use of CTN data collected with a medical CT scanner to estimate wood density, and a single calibration equation provides accurate wood density estimates for

values of MC varying from 6% to 117%. Therefore, we took subsamples from our air-dried wood disks after CT scanning and measured their MC. The average MC was 4.6, and the 95% confidence interval (2.8-6.4%) included 6%. Our CT-based wood density estimates were also calibrated with SilviScan-based wood density data (Manceur et al 2012; Appendix A).

To assess the directional variation in estimated wood density as well as the variation related to the size of the wood sample used for analysis, virtual wood cores were extracted digitally from the 3-D array of CTN data collected for each wood disk (Fig 1). This extraction was performed horizontally (in the *x*-*y* plane) in four orthogonal directions, ie along axes parallel to the *x* and *y* axes (both sides) and perpendicular to them passing through the center of the stem. The definition of a location for the center of the stem in a CT image was made graphically and numerically with a customized MATLAB (The MathWorks, Inc., Natick, MA) graphical unit interface, by zooming on the central part of the raw CT image. Each virtual wood core mimicked a cylinder of 1 voxel, 5 mm, or 12 mm in diameter, the latter two core sizes corresponding to the diameters of real wood cores usually extracted on-site from stems of standing trees in forest surveys. The customized MATLAB (The MathWorks) programs written by Dutilleul et al (2014) for virtual core extraction in their wood CT scanning study were used in this study (Appendix A). The directions of the *x* and *y* axes for a given wood disk are random relative to the geographical directions, because no mark had been made on the bark to indicate the north–south axis.

For each virtual wood core extracted (ie there are $3 \times 4 = 12$ for each of the eight white spruce trees sampled), a curve was produced from the estimated wood densities, approximately every 0.35 mm (ie the field of view or diameter of 18 cm, divided by 512) for small-size wood disks and approximately every 0.47 mm (ie 24 cm divided by 512) for medium-size wood disks. The beginning and end of the annual growth rings were identified from the interpeak distances in estimated wood density, following the calibration procedure of Manceur et al (2012; Appendix A), which was developed using raw measurements made with the SilviScan technology. As a basic complement, high-resolution (300 dpi) photographs of the wood disk surfaces were also used to count annual growth rings. The number of annual growth rings varied from 20 to 53 (excluding 2009, for which growth rings were incomplete) for the small-size wood disks and from 67 to 106 for the medium-size wood disks. To have some of the first years of growth for at least one white spruce tree in both groups, we selected the 18 calendar annual growth rings 1991-2008 for the five small-size wood disks

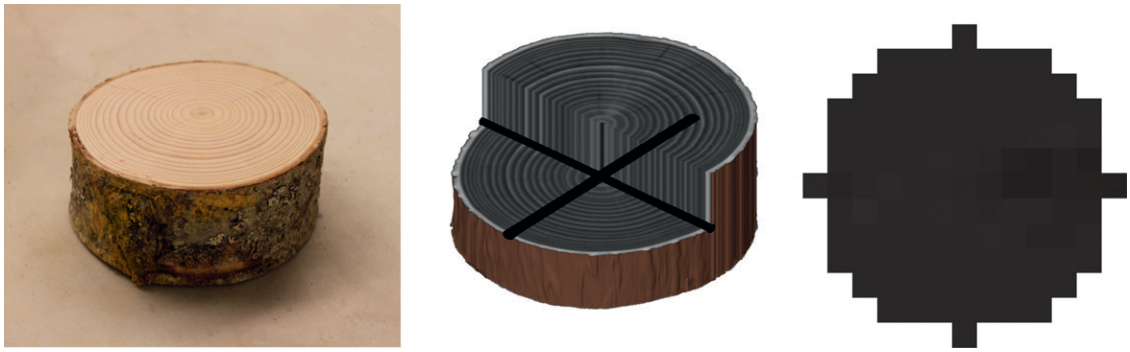

Figure 1. From left to right, a photograph of the small-size wood disk S1; an opened three-dimensional image of the same wood disk as reconstructed from computed tomography scanning data, in which four virtual wood cores with 5-mm diameter in orthogonal directions are represented by cylinders in dark gray (middle panel); and an exemplified two-dimensional image of the front of one of these cylinders.

and the 15 calendar annual growth rings 1950-1964 for the three medium-size wood disks for further data analyses.

Statistical Analysis

To determine if the core size, the direction from which the virtual wood core was extracted, or the year of growth statistically influenced, on its own or through an interaction, the mean value of wood densities estimated from CT scanning data, repeated-measures analyses of variance (ANOVAR) were performed with the general linear models procedure of SAS 9.3 (SAS 2010). The MIXED procedure was also tried with various variance–covariance structures, but because of convergence issues of the restricted maximum likelihood algorithm with the MIXED procedure in several cases, the general linear models procedure was retained. Because of the use of different fields of view in CT scanning, resulting in different levels of spatial resolution, and distinct periods of time, wood density estimates for small-size and medium-size wood disks were analyzed separately, using ANOVAR models with two fixed classification factors, core size and year of growth (crossed), and two random factors, tree and direction (nested within tree). Core size and year of growth were also both crossed with tree and direction (tree), allowing each ANOVAR model to include a total of three main effects, one nested effect, three interaction effects, and two error terms: one (Error 1) for the between-subject effects and another (Error 2) for the within-subject effects (Dutilleul 2011; Chapter 9).

Student t-tests for the comparison of two means from paired observations were performed for each of the 33 yr of growth that were studied (ie 1991-2008 for small-size wood disks and 1950-1964 for medium-size wood disks) to detect differences in mean wood density as estimated using virtual wood cores with diameters of 1 voxel, 5 mm, and 12 mm. Furthermore, the variance components associated with random effects (ie tree, direction [tree], year × tree, year × direction [tree]) and the experimental error for a given core size were estimated with SAS PROC VARCOMP.

RESULTS AND DISCUSSION

The radial patterns of estimated wood density for the three sizes of virtual wood cores are presented for the relevant periods for the five small-size wood disks and the three medium-size wood disks in Figs 2 and 3, respectively. The general radial trend for small-size wood disks shows that S2 had a slightly lower density on average (337.7 ± 21.2 kg/m^3), whereas S5 had a density (461.1 ± 11.8 kg/m^3) somewhat greater than that of the three other samples (∼400 kg/m^3). For medium-size wood disks, the estimated wood density ranged, on average, from 305.7 ± 28.1 kg/m^3 (M1) to 384.7 ± 12.4 kg/m^3 (M2) and 425.0 ± 13.6 kg/m^3 (M3). These estimates of wood density are in line with values reported for white spruce trees growing in natural stands (Jessome 1977). Among-tree differences represent by far the most important source of random variation in the data, before the year × direction (tree) and year-by-tree interactions, the direction (tree) effects and the experimental error in this order for the small-size wood disks and before the year-by-tree and year × direction (tree) interactions, the direction (tree) effects and the experimental error in this order for the medium-size wood disks for all three sizes of virtual wood core.

In Fig 2 (first panel), S1 shows a decreasing radial pattern that is different from the other small-size wood disks (S2-S5). According to Panshin and de Zeeuw (1980), such age-related wood density variation in conifers can be categorized in three general patterns, the first two being mainly seen in conifers growing in temperate and boreal regions. In Type-I pattern, the average wood density for a growth ring increased from the pith to the bark following a linear or curvilinear trend, flattening in the mature section. In Type-II pattern, the average wood density decreased for the first few growth rings, flattened in the next rings, and then increased until the mature period was reached. Although both types of patterns are encountered in white spruce, this tree species usually exhibits the Type-II pattern (Corriveau et al 1990; Lenz et al 2010). Possibly with the exception of S2, S1 was the only small-size wood disk

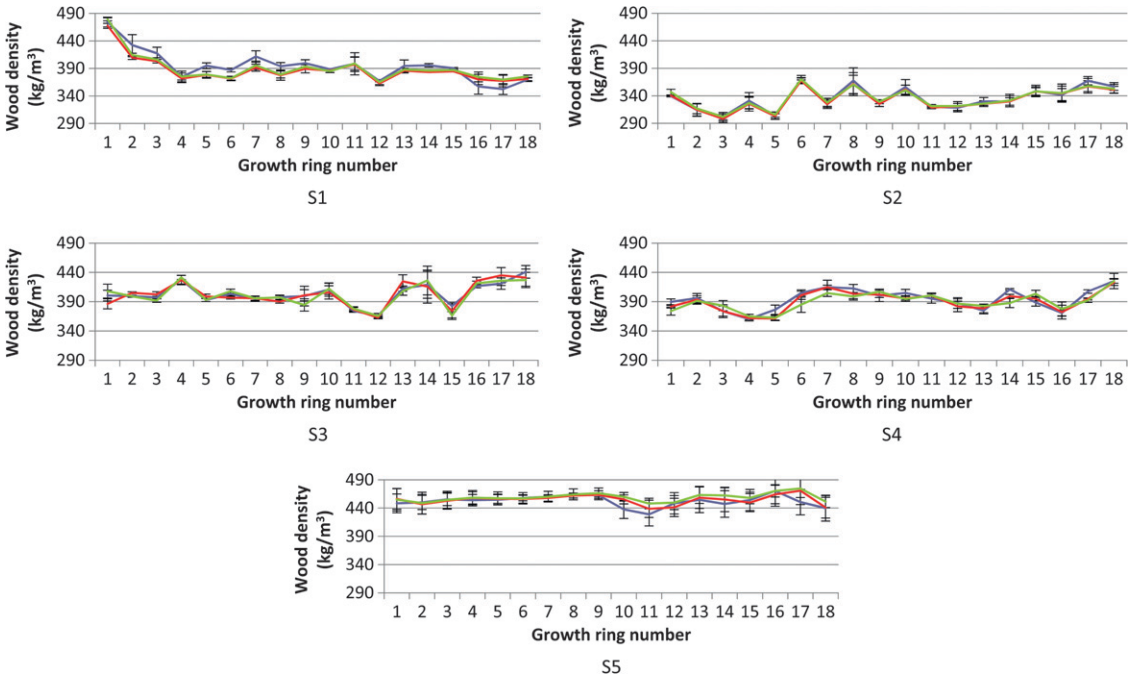

Figure 2. Radial patterns of wood density as estimated from computed tomography scanning data and averaged across the four orthogonal directions for five small-size wood disks from white spruce (*Picea glauca* [Moench] Voss) trees, shown for 18 yr (1991-2008) and for three virtual core diameters (1 voxel [blue], 5 mm [red], and 12 mm [green]).

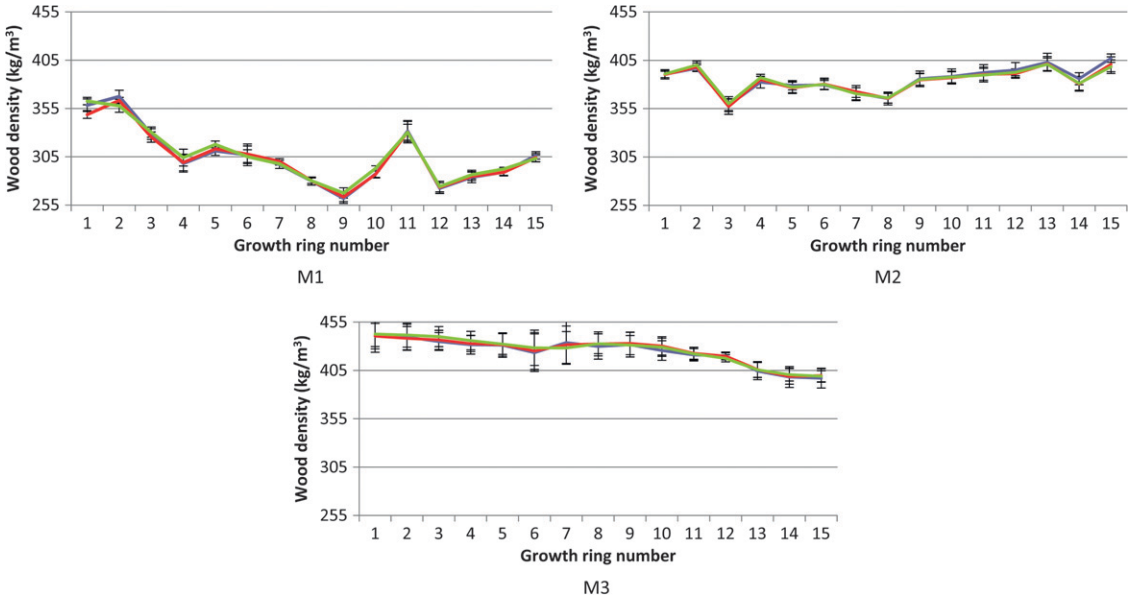

Figure 3. Radial patterns of wood density as estimated from computed tomography scanning data and averaged across the four orthogonal directions for three medium-size wood disks from white spruce (*Picea glauca* [Moench] Voss) trees, shown for 15 yr (1950-1964) and for three virtual core diameters (1 voxel [blue], 5 mm [red], and 12 mm [green]).

for which the first growth ring sampled for wood density estimation was sufficiently close to the pith to allow the observation of a decreasing radial pattern. Indeed, the cambial age of the first growth ring sampled for wood density estimation was 3, 6, 12, 14, and 36 yr in S1, S2, S3, S4, and S5, respectively. The wood density patterns of small-size disks S3 and S4 appeared to be representative of the transition zone between juvenile and mature woods, in which density flattens and starts to increase as the trees mature. The small-size disk S5, for which we present estimated wood densities in growth rings 36 to 53 from the pith, was mainly made of mature wood, and it is very interesting that these estimated wood densities were greater than those for other small-size wood disks and were almost flattening.

In the radial patterns of estimated wood density for the three medium-size wood disks (Fig 3), the first of the 15 sampled growth rings corresponded to a cambial age of 9, 16, and 48 yr for M1, M2, and M3, respectively. The radial patterns of estimated wood densities for M1 and M2 suggest a transition zone in which wood density starts to increase after having decreased across a small number of growth rings from the pith. Interestingly, the radial patterns of estimated wood density for small-size and medium-size wood disks were similar when the cambial age of annual rings was in the same range (S3 and S4 vs M1 and M2). However, the radial pattern observed for M3 is different from what was observed with small-size wood disks, even if the cambial age of the annual rings that were sampled was close to what it was for S5. Indeed, the estimated wood density for M3 decreased from the first experimental growth ring (1950, cambial age of 48 yr) to the last one (1964, cambial age of 62 yr). Although the cambium of that tree was not very old, it clearly showed a trend similar to those observed in overmature trees, in which wood density exhibited a slight decrease in outer rings.

Various factors can affect wood density and its radial pattern, but the following three factors may be considered the most important: 1) weather conditions of the growing season, via their influence on the corresponding growth of the tree crown and stem and the wood produced (Larson 1962); 2) competition between the tree and its neighbors, which favors self-pruning of lower branches, and the resulting hormonal gradients, which influence the xylem development (distance from the living crown) (Larson 1969); and 3) aging of the cambium, which induces variation in the secondary tissues (distance from the pith) (Panshin and de Zeeuw 1980). Diverging weather and competition conditions probably explain why the radial patterns of estimated wood densities for M3 and S5 in this study were different, despite similar cambial age ranges. Unfortunately, climatic and competition data were not available to disentangle which of these two factors might be more influential. The three factors previously mentioned, as well as others, undoubtedly had an effect on the high variability among trees, observed in the wood disks analyzed here.

Another interesting finding of this study is that CT scanning provides data that can be used to estimate wood densities and obtain radial patterns similar to those obtained with other technologies, such as X-ray densitometry. Furthermore, both the estimated wood densities themselves and the variation in the derived radial patterns are in line with reported data (Jessome 1977) and the types of patterns expected and described by Panshin and de Zeeuw (1980).

The radial patterns of estimated wood densities for most of the wood disks in Figs 2 and 3 show large standard errors for a large number of the annual rings. This is a clear indication that in those years, wood density varied substantially among the four orthogonal directions along which virtual wood cores were extracted and that the CT scanning technology can capture that variation. Results of the ANOVAR show, indeed, that differences related to the direction of extraction are statistically significant (Tables 1 and 2). Nevertheless, variation caused by direction is generally not considered when sampling trees, because it is small relative to the among-tree variation. Past research has shown, however, that multiple core

Table 1. Repeated-measures analysis of variance for wood densities estimated from computed tomography scanning data collected for small-size white spruce wood disks.

Source of variation	F	*p* value
Between-subject effects		
Core size	1.33	0.2754
Tree	80.93	<0.0001
Direction (tree)	20.56	<0.0001
Error 1		
Within-subject effects		
Year	40.84	<0.0001
Year × core size	0.83	0.6197
Year × tree	4.39	<0.0001
Year × direction (tree)	11.61	<0.0001
Error 2		

Table 2. Repeated-measures analysis of variance for wood densities estimated from computed tomography scanning data collected for medium-size white spruce wood disks.

Source of variation	F	*p* value
Between-subject effects		
Core size	0.71	0.5024
Tree	123.43	<0.0001
Direction (tree)	73.12	<0.0001
Error 1		
Within-subject effects		
Year	363.22	<0.0001
Year × core size	1.44	0.1742
Year × tree	8.89	<0.0001
Year × direction (tree)	30.00	<0.0001
Error 2		

sampling could improve the precision of wood density estimation (Taras and Wahlgren 1963), at the expense of higher costs. Many studies (Wahlgren and Fassnacht 1959; Wahlgren et al 1966; Brazier and Howell 1979) have also shown high positive correlation between single breast-height and multiple whole-tree wood density estimates, and this is why wood density estimated from one core collected at breast height is generally considered to be representative of the whole tree (Gonzalez 1990). Nevertheless, a better precision in wood density estimates can be obtained by using several cores, real or virtual, per tree.

At the 10% significance level, Student t-tests for paired comparisons of virtual wood core sizes led to ~15% significant differences for small-size wood disks at the beginning of the studied period for the diameters of 5 and 12 mm (1991, 1994, 2002), more than approaching the end for the 1-voxel-to-5-mm-diameter comparison (1998, 2002, 2003, 2008), and for only 1 yr in between (1998) for the 1-voxel-to-12-mm-diameter comparison. For medium-size wood disks, there was ~13% significant difference between core sizes, mainly for the 5- and 12-mm diameters (1950, 1956, 1959, 1963) and to a lesser degree in 1-voxel-to-12-mm-diameter comparisons (1953, 1959); no significant difference was found between the 1-voxel and 5-mm diameters. Although they are clearly and correctly reflected through the age effects in radial patterns of estimated wood density (see the highly significant tree main effects and year × tree interaction in Tables 1 and 2), the very large among-tree differences in both groups of wood disks may explain at least in part the relative lack of significance of the effects related to virtual wood core size (see the core size main effects in Tables 1 and 2 and the paired comparisons year by year).

When wood density is estimated from cores collected from stems of standing trees, one may expect that cores with larger diameter (eg 12 mm) cause less wood compaction because the area-to-volume ratio of the wood sample is smaller and that they are easier to process and analyze (Williamson and Wiemann 2010). The collection of real wood cores is complicated by the fact that larger cores can also have greater distortions because of the increased force used in their extraction, particularly for large trees. However, cores obtained using hydraulic drills are superior to those obtained manually. In this study, such potential biases related to the size of the wood core did not exist because of the virtual nature of the wood cores, extracted digitally on computer from the collected CT scanning data. This is another possible reason for the absence of statistically significant effects of Core size (Tables 1 and 2).

CONCLUSIONS

In this study, high-resolution data were collected on wood disks by CT scanning and a calibration

equation was used to obtain estimates of wood density. Proceeding in this way, it was possible to extract, digitally on computer, virtual wood cores of various sizes in four orthogonal directions. With the wood density estimates thus obtained, radial patterns were delineated and hypotheses about direction, core size, year of growth and their interactions were tested. The observed radial patterns of estimated wood density are typical of the patterns traditionally reported for white spruce in the literature. With experimental trees being of different ages, a large among-tree variation was observed, together with a less important, although statistically significant, variation within a wood disk associated with the direction in which a virtual wood core was extracted. It was not possible to demonstrate effects caused by core size. CT scanning technology allows the rapid 3-D collection of millions of CT numbers on wood disks. Subsequently, after processing, it is possible to test a broad variety of hypotheses with regards to variation in wood traits, in particular wood density.

ACKNOWLEDGMENTS

We are grateful to S. Clement for his review of a preliminary version of the manuscript and to P. Cheers for her editing work. We also gratefully acknowledge the financial assistance of the Canadian Wood Fibre Centre through a research grant to J. Beaulieu and of the Natural Sciences and Engineering Research Council of Canada through a Discovery Grant to P. Dutilleul.

REFERENCES

Baltunis BS, Wu HX, Powell MB (2007) Inheritance of density, microfibril angle, and modulus of elasticity in juvenile wood of *Pinus radiata* at two locations in Australia. Can J For Res 37:2164-2174.

Beaulieu J (2003) Genetic variation in tracheid length and relationships with growth and wood traits in eastern white spruce (*Picea glauca*). Wood Fiber Sci 35:609-616.

Beaulieu J, Doerksen T, Boyle B, Clément S, Deslauriers M, Beauseigle S, Blais S, Poulin P-L, Lenz P, Caron S, Rigault P, Bicho P, Bousquet J, MacKay J (2011) Association genetics of wood physical traits in the conifer white spruce and relationships with gene expression. Genetics 188:197-214.

Beaulieu J, Doerksen TK, MacKay J, Rainville A, Bousquet J (2014) Genomic selection accuracies within and between environments and small breeding groups in white spruce. BMC Genomics 15:1048.

Brazier JD, Howell RS (1979) The use of breast-height core for estimating selected whole-tree properties of Sitka spruce. Forestry 52:177-185.

Bucur V (2003) Nondestructive characterization and imaging of wood. Springer, New York, NY.

Corriveau A, Beaulieu J, Daoust G (1991) Heritability and genetic correlations of wood characters of Upper Ottawa Valley white spruce populations grown in Quebec. For Chron 67:698-705.

Corriveau A, Beaulieu J, Mothe F, Poliquin J, Doucet J (1990) Densité et largeur des cernes des populations d'épinettes blanches de la région forestière des Grands Lacs et du Saint-Laurent. Can J For Res 20:121-129.

Cown D, McConchie D, Young G (1991) Radiata pine—Wood properties survey. FRI Bull 78:45-58.

Dutilleul P (2011) Spatio-temporal heterogeneity: Concepts and analyses. Cambridge University Press, Cambridge, UK.

Dutilleul P, Han L, Beaulieu J (2014) How do trees grow? Response from the graphical and quantitative analyses of computed tomography scanning data collected on stem sections. Comment les arbres poussent-ils? Réponse des analyses graphique et quantitative de données de tomodensitométrie pour des sections de la tige. C R Biol 337:391-398.

Evans R, Ilic J (2001) Rapid prediction of wood stiffness from microfibril angle and density. Forest Prod J 51:53-57.

Freyburger C, Longuetaud F, Mothe F, Constant T, Leban J-M (2009) Measuring wood density by means of X-ray computer tomography. Ann Sci 66:804-812.

Gonzalez JS (1990) Wood density of Canadian tree species. Forestry Canada, Edmonton, AB, Canada, Inf Rep NOR-X-315.

Han L, Dutilleul P, Prasher SO, Beaulieu C, Smith DL (2008) Assessment of common scab-inducing pathogen effects on potato underground organs via computed tomography scanning. Phytopathology 98:1118-1125.

Ivkovich M, Namkoong G, Koshy M (2002a) Genetic variation in wood properties of interior spruce. I. Growth, latewood percentage, and wood density. Can J For Res 32:2116-2127.

Ivkovich M, Namkoong G, Koshy M (2002b) Genetic variation in wood properties of interior spruce. II. Tracheid characteristics. Can J For Res 32:2128-2139.

Jessome AP (1977) Strength and related properties of woods grown in Canada. For Tech Rep 21. Environ Can, Can For Serv East Forest Prod Lab, Ottawa, Ontario.

Kalender WA (2000) Computed tomography. Publicis MCD Verlag, Munich, Germany.

Kibblewhite RP (1999) Designer fibres for improved papers through exploiting genetic variation in wood microstructure. Appita J 52:429-435.

Kumar S, Dungey HS, Matheson AC (2006) Genetic parameters and strategies for genetic improvement of stiffness in radiata pine. Silvae Genet 55:77-84.

Larson PR (1962) A biological approach to wood quality. TAPPI 45:443-448.

Larson PR (1969) Wood formation and the concept of wood quality. Bull 74, Yale University, School of Forestry, New Haven, CT. 54 pp.

Larson PR (1994) The vascular cambium: Development and structure. Springer-Verlag, Berlin, Germany.

Lenz P, Cloutier A, MacKay J, Beaulieu J (2010) Genetic control of wood properties in *Picea glauca*—An analysis of trends with cambial age. Can J For Res 40:703-715.

Lenz P, Deslauriers M, Ung C-H, MacKay J, Beaulieu J (2014) What do ecological regions tell us about wood quality? A case study in eastern Canadian white spruce. Can J For Res 44:1383-1393.

Lenz P, MacKay J, Rainville A, Cloutier A, Beaulieu J (2011) The influence of cambial age on breeding for wood properties in *Picea glauca*. Tree Genet Genomes 7:641-653.

Lindgren LO (1991) The accuracy of medical CAT-scan images for non-destructive density measurements in small volume elements within solid wood. Wood Sci Technol 25:425-432.

MacDonald E, Hubert J (2002) A review of the effects of silviculture on timber quality of Sitka spruce. Forestry 75:107-138.

MacKenzie J, Bruemmer G (2009) Enhancing Canada's forest fibre. For Chron 85:353-354.

Manceur AM, Beaulieu J, Han L, Dutilleul P (2012) A multidimensional statistical model for wood data analysis, with density estimated from CT scanning data as an example. Can J For Res 42:1038-1049.

Myszewski JH, Bridgwater FE, Lowe WJ, Byram TD, Megraw RA (2004) Genetic variation in the microfibril angle of loblolly pine from two test sites. South J Appl For 28:196-204.

Panshin AJ, de Zeeuw C (1980) Textbook of wood technology: Structures, identification, properties and uses of the commercial woods of the United States and Canada. 4th ed. McGraw-Hill Book Company, New York, NY. 722 pp.

Plomion C, Leprovost G, Stokes A (2001) Wood formation in trees. Plant Physiol 127:1513-1523.

SAS (2010) SAS/STAT software, SAS Institute Inc. Version 9. 3. Cary, NC.

Sinnott EW (1952) Reaction wood and the regulation of tree form. Am J Bot 39:69-78.

Taras MA, Wahlgren HE (1963) A comparison of increment core sampling methods for estimating tree specific gravity. Res Pap SE-7 USDA For Serv Southern Forest Exp Stn, Asheville, NC.

UK Forest Commission (2005) Compression wood in conifers—The characterisation of its formation and its relevance to timber quality. Final Report. 376 pp. http://www.forestry.gov.uk/compressionwood (17 April 2016).

Upton B, Miner R, Spinney M, Health LS (2008) The greenhouse gas and energy impacts of using wood instead of alternatives in residential construction in the United States. Biomass Bioenerg 32:1-10.

Wahlgren HE, Fassnacht DL (1959) Estimating tree specific gravity from a single increment core. Rep No 2146 USDA For Serv Forest Prod Lab, Madison, WI.

Wahlgren HE, Hart AC, Maeglin RR (1966) Estimating tree specific gravity of Maine conifers. Res Pap 27 USDA For Serv Forest Prod Lab, Madison, WI.

Williamson GB, Wiemann MC (2010) Measuring wood specific gravity. . .Correctly. Am J Bot 97:519-524.

Yanchuk AD, Kiss GK (1993) Genetic variation in growth and wood specific gravity and its utility in the improvement of interior spruce in British Columbia. Silvae Genet 42:141-148.

Zobel BJ, van Buijtenen JP (1989) Wood variation: Its causes and control. Springer-Verlag, New York, NY. 363 pp.

APPENDIX A

Extraction of virtual wood cores from three-dimensional (3-D) wood computed tomography (CT) scanning data and calculation of ordinates in curves of estimated wood densities with MATLAB (The MathWorks Inc.)

In this appendix are grouped a number of more technical, computational details which, if they had been presented in the body of the article, would have disrupted the presentation of materials there. Their inclusion here is justified because they convey information that is likely to be useful to readers in their future work with wood samples and a CT scanner.

PROCESSING OF VIRTUAL WOOD CORES AND COMPUTATION OF MEAN ESTIMATED WOOD DENSITIES

Definition of some of the variables:

WoodCTScanData: 3-D array containing the CT numbers collected for the wood sample (eg section of the stem; Fig 1, left panel) that has been CT scanned.

D: diameter (in voxels) of the cylinder that mimics a wood core, eg 13 (Fig 1, right panel) if the diameter in centimeters is 5 and the CT scanning resolution is such that the pixel dimensions of a pixel in the *x-y* plane of CT scanning is 0.35×0.35 mm.

R: radius (in voxels) of the cylinder, ie $R = 0.5 \times D$.

L: cylinder length (in voxels), across which wood density is estimated at each voxel from wood CT scanning data contained in the cylinder.

```
function [Core WoodCoreDensity] = Wood-
Core(WoodCTScanData,D,Theta,Starting-
Point,L)

% This program outputs a vector of esti-
mated wood densities for a virtual core
with diameter D and length L (called "the
cyclinder" in the definitions above), in
one of four orthogonal directions for one
tree (below, for an angle Theta of zero
degree relative to a direction of reference,
e.g. the X-axis of CT scanning; other values
of Theta: 90, 180, 270 degrees).

Core=Cylinder_Maker(WoodCTScanData,
StartingPoint,D,L,Theta);

Core_Dir=Core(StartingPoint(1):
StartingPoint(1)+L-1,StartingPoint(2)-R:
StartingPoint(2)+R,StartingPoint(3)-R:
StartingPoint(3)+R);

Core=X_Y_Z_Rotation(Core_Dir);

% The three lines of code above perform the
extraction of a cylindrical virtual wood
core with dimensions D and L from the 3-D
array WoodCTScanData (Figure 1, middle
panel); this core is oriented in accordance
with StartingPoint and Theta; and rota-
tions are applied as necessary.

WoodCoreDensity=AVG_Profile(Core);

% This line calls the function AVG_Profile
to calculate the mean estimated wood
density at each voxel along the central
axis of the virtual core. That is, from all
the estimated wood densities available for
the cross-section of the cylinder at the
voxel considered along the axis, an average
is calculated and used as ordinate of the
curve to be plotted over length L.
```

CONSTRUCTION OF CYLINDRICAL VIRTUAL WOOD CORES

```
function Cylinder=Cylinder_Maker(Wood-
CTScanData,StartingPoint,D,L,Theta)

% This function, which is called in the
WoodCore function, builds up a cylinder
with diameter D and length L, from the
specified StartingPoint in the data array
WoodCTScanData. Accordingly, the vari-
ables WoodCTScanData, StartingPoint, D,
L, and Theta have the same definitions and
meanings as above.

[r c p] =Size(WoodCTScanData);

Cylinder_BW=false(r,c,p);

X=StartingPoint(1);

Y=StartingPoint(2);

Z=StartingPoint(3);

R=floor(D/2);
```

```
if Theta==0
for k=Z-R:Z+R
for j=Y-R:Y+R
for i=X:X+L-1
if ((k-Z)^2+(j-Y)^2)<=(R)^2
Cylinder_BW(i,j,k)=1;
end
end
end
end
Cylinder=int16(Cylinder_BW).*WoodCT-
ScanData;
```